

Design and synthesis of novel p-type transparent solar thin film  
with CuGaO<sub>2</sub> nanoparticle

Undergraduate Research Thesis

Presented in partial fulfillment of the requirements for graduation with Honors Research  
Distinction in Chemistry in the undergraduate college of The Ohio State University

By

Shengchen Xue

Undergraduate Program in Chemistry

The Ohio State University

2016

Thesis Committee:

Prof. Yiyang Wu

Copyright by

Shengchen Xue

2016

## Abstract

CuGaO<sub>2</sub>, a p-type transparent semiconductor, have a great potential to be used in various electronics, such as p-type dye-sensitized solar cell, since it has a high carrier mobility, approximately  $10^{-2}$ - $10\text{ cm}^2\text{ V}^{-1}\text{ s}^{-1}$ , and large optical bandgap, 3.4-3.7 eV. The purpose of this research is to develop an accessible approach to fabricate the CuGaO<sub>2</sub> thin film at low cost. By studying the hydrothermal synthesis of CuGaO<sub>2</sub>, two recipes are established to produce the CuGaO<sub>2</sub> nanoparticles with diameters of 200 nm and 5  $\mu\text{m}$ . Also it has been found that the CuGaO<sub>2</sub> nanoparticles of different dimensions have different colors. The 200 nm nanoparticle is grey while the 5  $\mu\text{m}$  particle is yellow. To make the CuGaO<sub>2</sub> thin film, 200 nm nanoparticle is mainly used in both the self-assembly approach and electro-spraying technique. Although, based on thermodynamics, self-assembly is a theoretically possible way to make single layer thin film, the actual films made through this process have very poor morphologies due to the amalgamation and non-even distribution of the CuGaO<sub>2</sub> nanoparticles. The electro-spraying technique, a physical deposition process, can give much better morphology of the thin film. Samples made though the electro-spraying process can have a locally perfect morphology with thickness of approximately 500 nm, but the morphology of the whole film is still defective, containing holes and vacancies. Therefore, the electro-spraying process still need to be studied based on the established physical model to discover more suitable experimental-parameters.

## Dedication

Dedicated to my mother and father

## Acknowledgments

I would like to thank Prof. Yiying Wu for his approval, support, and advice of this project. I would thank Dr. Mingze Yu for mentoring.

Also, this project is help by Prof. Jianjun Guan and two of his PhD. Candidates, Xiaofei Li and Bo Zhao, with the experiment setup of the electro-spraying technique.

## Vita

August 2013 – present ..... The Ohio State University

## Field of Study

Major Field: Materials Science and Engineering

## Table of Contents

Abstract .....	ii
Dedication .....	iii
Acknowledgments .....	iv
Vita .....	v
Table of Contents .....	vi
List of Tables .....	viii
List of Figures .....	ix
Chapter 1: Overview .....	1
1.1 Motivation .....	1
1.2 Introduction .....	2
Chapter 2: Approaches and Methodologies .....	5
2.1 Synthesis of CuGaO <sub>2</sub> particles .....	5
2.2 Colloid formation .....	8
2.3 Fabrication of CuGaO <sub>2</sub> thin film through electro-spraying process .....	11
2.4 Fabrication of CuGaO <sub>2</sub> thin film through self-assembly .....	15
Chapter 3: Results and Discussion .....	17
3.1 CuGaO <sub>2</sub> thin film fabricated through electro-spraying .....	17
3.2 CuGaO <sub>2</sub> thin film fabricated through self-assembly .....	21
Chapter 4: Conclusion .....	23
Chapter 5: Future Work .....	24
References .....	25
Appendix A: Microscopic image of CuGaO <sub>2</sub> thin film .....	26

Appendix B: Image analysis of Figure 13 .....	27
---	----



## List of Tables

<b>Table 1:</b> Relationship between the usage of CuGaO <sub>2</sub> particles and coverage .....	19
---	----

## List of Figures

<b>Figure 1:</b> Crystal structure of CuGaO <sub>2</sub> , (a) Rhombohedra, (b) Hexagonal.....	3
<b>Figure 2:</b> (a) SEM image of 200 nm CuGaO <sub>2</sub> nanoparticles, (b) Optical microscopic image of 5 μm CuGaO <sub>2</sub> nanoparticles.....	6
<b>Figure 3:</b> Schematic of electrical double layer .....	9
<b>Figure 4:</b> CuGaO <sub>2</sub> colloid.....	11
<b>Figure 5:</b> (a) Setup of electro-spraying, (b) Schematic of electro-spraying .....	12
<b>Figure 6:</b> Schematic of electric field of the electro-spraying process.....	14
<b>Figure 7:</b> (a) appearance of sample made though electro-spraying, (b) SEM image of the first sample made though electro-spraying (without using CuGaO <sub>2</sub> colloid) .....	17
<b>Figure 8:</b> CuGaO <sub>2</sub> thin film made though electro-spraying by using colloid .....	18
<b>Figure 9:</b> (a) Morphology of locally-fully covered thin film (FTO substrate), (b) Simulation of thin film, (c) thickness data of thin film.....	20
<b>Figure 10:</b> Morphology of locally-fully covered thin film (ITO substrate).....	20
<b>Figure 11:</b> (a)-(d) Samples made though self-assembly .....	22
<b>Figure 12:</b> Morphology of thin film with different amount of CuGaO <sub>2</sub> nanoparticles, (a) 0.007g, (b) 0.015 g, (c) 0.022g, (d) 0.030 g, (e) 0.038g, (f) 0.046 g, (g) 0.054 g.....	26
<b>Figure 13:</b> Image process of Figure 13. (black: covered, white: uncovered) .....	27

## Chapter 1: Overview

### 1.1 Motivation

Due to the severe environmental issues caused by the combustion of fossil fuel, the exploration of alternative energies is critical. In recent years, solar photovoltaic energy has been studied as one of the most promising alternative sources. Transparent solar thin films have been a large focus in these studies. In contrast to the traditional rigid solar panels composed of crystalline silicon, transparent solar thin films are more lightweight and flexible, as well as being transparent. Therefore, they can be used in a wider range of applications.

The mechanisms of transparent solar thin films rely on the formation of p-n junctions, where both p-type material and n-type material are used (Kassap, 2012). Due to the intrinsic properties of materials, there is a significant disparity between the developments of p-type and n-type transparent thin film materials. The candidates of the n-type materials are abundant, but only a few possible p-type materials have been discovered.

Delafossite ( $\text{CuGaO}_2$ ) is a p-type transparent conducting oxide that can be used for both fundamental science and industrial applications, especially for dye-sensitized

solar cells. It has better electrical conductivity than the commonly used NiO-based p-type semiconductors. Conventional syntheses of CuGaO<sub>2</sub> include solid-state reaction and vacuum-deposition methods. Both techniques have limitations. Solid-state reaction requires high temperature sintering and yield amalgamated particles that are typically larger than 1 μm. Vacuum deposition techniques require fastidious experiment conditions. A hydrothermal synthesis method is conceived as a more technically-accessible and economical method for acquiring CuGaO<sub>2</sub> nanoparticles (Draskovic et al., 2014).

The current existing methodologies applied to make the thin films include pulsed laser deposition, sol-gel precursor-calcination, and high temperature synthesis. All of these three methods require vacuum condition and a high temperature greater than 1000 C°. This contributes to a high manufacturing cost. Therefore, the electro-spraying technique and self-assembly method are studied to fabricate high quality CuGaO<sub>2</sub> thin films at low cost.

## 1.2 Introduction

The objective of this project is to study and develop techniques to form the CuGaO<sub>2</sub> thin film at low cost. CuGaO<sub>2</sub>, as reported by Draskovic et al. (2014), has a rhombohedra or hexagonal crystal structure as shown in Figure 1. Also, because of the defects of the crystal structure of CuGaO<sub>2</sub>, Cu vacancies and O interstitials, it is a p-type material with a hole-mobility of approximately  $10^{-2}$ - $10 \text{ cm}^2 \text{ V}^{-1} \text{ s}^{-1}$  (Nie et al., 2002, Fang et al., 2008, and Gillen &Robertson, 2011). According to Nie et al. (2002), the valence band edge of CuGaO<sub>2</sub>, which has been studied both experimentally and theoretically, is

about 5.1 eV below the vacuum level, and the bandgap of this material is within 3.4-3.7 eV (Benko & Koffyberg, 1986, and Ueda et al., 2001). Due to its high carrier mobility and large optical bandgap, CuGaO<sub>2</sub> is a promising material for assorted electronic applications, such as p-n junctions and p-type dye-sensitized solar cell (Ji et al., 2012).

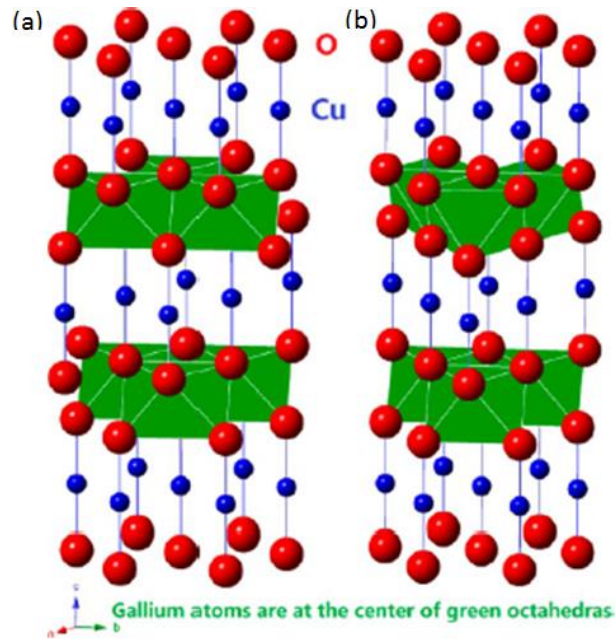


**Figure 1:** Crystal structure of CuGaO<sub>2</sub>, (a) Rhombohedra, (b) Hexagonal

As the hydrothermal synthesis process has been developed, the production of CuGaO<sub>2</sub> nanoparticles at low cost is no longer a problem. However, fabricating thin film with the preexisting CuGaO<sub>2</sub> nanoparticles becomes a challenging issue for the applications of this material, because commonly used techniques to fabricate high quality films, such as chemical vapor deposition and spinning coating, which all involve

nucleation and grain growth of materials, are not applicable in this case. Hence, physical deposition becomes the most suitable choice in this situation. Nevertheless, commonly used physical deposition techniques, such as physical vapor deposition, sputtering, and pulsed laser deposition, contradict the idea of low-cost fabrication. Therefore, the self-assembly process, which uses thermodynamics, and the electro-spraying technique, established on the model of electro-spinning, are conceived and tested as easy techniques to fabricate the  $\text{CuGaO}_2$  thin films with the hydrothermally synthesized nanoparticles.

## Chapter 2: Approaches and Methodologies

### 2.1 Synthesis of CuGaO<sub>2</sub> particles

The CuGaO<sub>2</sub> nanoparticles is hydrothermally synthesized by using Cu(NO<sub>3</sub>)<sub>2</sub> and Ga(NO<sub>3</sub>)<sub>3</sub> as precursors and potassium hydroxide as a mineralizer. According to Draskovic et al. (2014), the temperature of this process need to be set greater than 180 °C and the pH value is tuned to values between 3.4 to 6.6 by adding K(OH). Both the experiment temperature and pH value are critical for the purity and morphology of the final CuGaO<sub>2</sub> product. Moreover, if smaller nanoparticles are needed, surfactant, such as CTAB, can be added to inhibit the grain growth of the CuGaO<sub>2</sub> nanoparticles.

For this research two recipes are applied to synthesize CuGaO<sub>2</sub> nanoparticles with different sizes, diameters of 200 nm and 5 µm, as shown in Figure 2. Nanoparticles with diameter of 200 nm are grey and the color of the 5 µm nanoparticles is yellow.

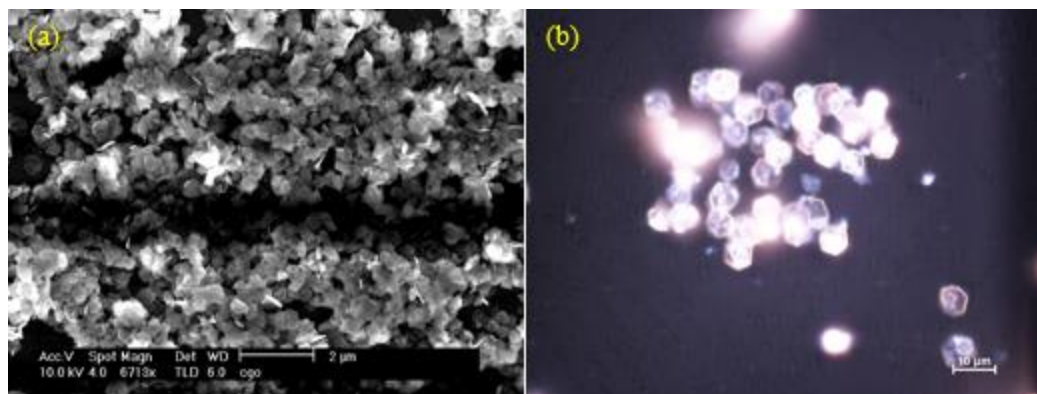


**Figure 2:** (a) SEM image of 200 nm CuGaO<sub>2</sub> nanoparticles, (b) Optical microscopic image of 5 μm CuGaO<sub>2</sub> nanoparticles

Based on Draskovic et al. (2014), recipe and procedure used to synthesize the 200 nm CuGaO<sub>2</sub> nanoparticles are:

- Cu(NO<sub>3</sub>)<sub>2</sub>: 0.1159 g
  - Ga(NO<sub>3</sub>)<sub>3</sub>: 0.1919 g
  - CTAB: 0.05 g
- } + 6 mL H<sub>2</sub>O
- Tune pH to 6.37 by using KOH (0.134 g + 6 mL H<sub>2</sub>O)
  - 2 mL ethylene glycol (EG)
  - Stir for 12 hours
  - Heat for 52 hours at 193 °C



The recipe used to synthesize the bigger particles is based on the idea of Cario et al. (2008):

- $\text{Cu}(\text{NO}_3)_2$ : 0.1116 g
  - $\text{Ga}(\text{NO}_3)_3$ : 0.1799 g
- } +6 mL  $\text{H}_2\text{O}$
- Tune pH to 5.5 by using KOH (0.134 g + 6 mL  $\text{H}_2\text{O}$ )
  - 2 mL ethylene glycol (EG)
  - Stir for 12 hours
  - Heat for 52 hours at 193 degree Celsius

In both recipes EG is used as the reduce agent to reduce the  $\text{Cu}^{2+}$  to  $\text{Cu}^{1+}$ , but the second recipe does not include CTAB which is used in the first synthesis as surfactant to assist the production of smaller nanoparticles. The two recipes also vary in their pH value. For the second synthesis process, 0.48 mmol of  $\text{Cu}(\text{NO}_3)_2$  and  $\text{Ga}(\text{NO}_3)_3$  are used, and, to achieve the final pH value, 2.40 mmol of  $\text{K}(\text{OH})$  is added to fully precipitate the  $\text{Cu}^{2+}$  and  $\text{Ga}^{3+}$ .

Potential impurities for both synthesis processes are  $\text{Cu}_2\text{O}$  and  $\text{GaOOH}$ , so the product can be purified by using diluted ammonium hydroxide ( $\text{NH}_4\text{OH}$ ). By applying the XRD analysis, the majorly used two recipes are testified to be able produce nearly 100% pure  $\text{CuGaO}_2$ .

## 2.2 Colloid formation

The CuGaO<sub>2</sub> colloid is made especially for the electro-spraying process. Because, by definition, colloid is consist of the dispersed-phase particles with diameter between 1 to 1000 nm (Levine, 2001), only the 200 nm CuGaO<sub>2</sub> particles are used to make the colloid. By mixing 0.008 g CuGaO<sub>2</sub> with 2.99 mL ethanol and 0.01 mL HCl which has a pH of 1, a basic CuGaO<sub>2</sub> colloid is formed and it can be stable for several hours.

The basic idea applied for the colloid formation is to make use of the electrical double layer. The surface of CuGaO<sub>2</sub>, an oxide, is most likely to have oxygens which are negatively charged, so when CuGaO<sub>2</sub> is put into a weak acid condition, in this specific case mixture of 2.99 mL ethanol with 0.01 mL HCl of pH 1, the H<sup>+</sup> will be attracted by the O<sup>2-</sup> on the surface of CuGaO<sub>2</sub> nanoparticles as shown in the following schematic, Figure 3. Hence, some H<sup>+</sup> will closely bond with the surface of the CuGaO<sub>2</sub> nanoparticles, forming the stern layer, while some H<sup>+</sup> will be around the CuGaO<sub>2</sub> nanoparticles, creating a diffuse layer. Because the surface of each individual CuGaO<sub>2</sub> nanoparticle has the same charge, particles will repel each other, preventing the formation of the amalgamations.

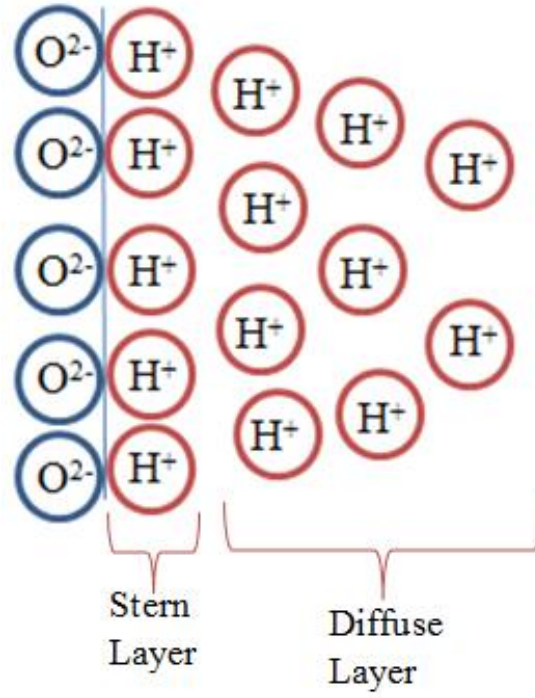


**Figure 3:** Schematic of electrical double layer

Based on this model, the density of ions on the particle surface can be calculated by:

$$C_s = C_{zp} \cdot e^{-Ze\psi_s/k_B T}$$

where  $C_s$  is the charge density of ions on the surface,  $C_{zp}$  is the zero point charge density,  $Ze$  gives the charges on the surface,  $\psi_s$  is the surface potential,  $k_B$  is the Boltzmann constant, and  $T$  is the temperature.

To find the electrostatic potential in the double layer, Poisson-Boltzmann equation is used, and the derivation is shown below:

$$\begin{aligned}\nabla \cdot \vec{D} &= \rho \\ \varepsilon_0 \varepsilon_r \frac{dE}{dx} &= \rho \\ -\varepsilon_0 \varepsilon_r \frac{d^2\psi}{dx^2} &= \sum_i Z_i e n_{0i} \exp\left(-\frac{Z_i e \psi}{k_B T}\right)\end{aligned}$$

where  $\vec{D}$  is the electric displacement,  $\rho$  is the local charge density,  $\varepsilon_0$  is the electric permittivity of free space,  $\varepsilon_r$  is the relative permittivity,  $E$  is the electric field,  $\psi$  is the electrostatic potential,  $Z_i e$  is the charge of a certain species per ion, and  $n_{0i}$  is the ion density of a certain species at infinity.

Based on the rational of electrical double layer, the colloid is made as shown in Figure 4.



**Figure 4:** CuGaO<sub>2</sub> colloid

### 2.3 Fabrication of CuGaO<sub>2</sub> thin film through electro-spraying process

The self-designed electro-spraying process is conceived based on the concept of the electro-spinning technique which is a widely-used modern technique for making polymer scaffolds. Greiner and Wendorff (2007) explain the main working mechanism is to make use of the collaborative effect of electrostatic repulsion between the polarized organic solvent and the columbic force generated by the external electric field. The experimental setup and a schematic of this process are shown Figure 5:

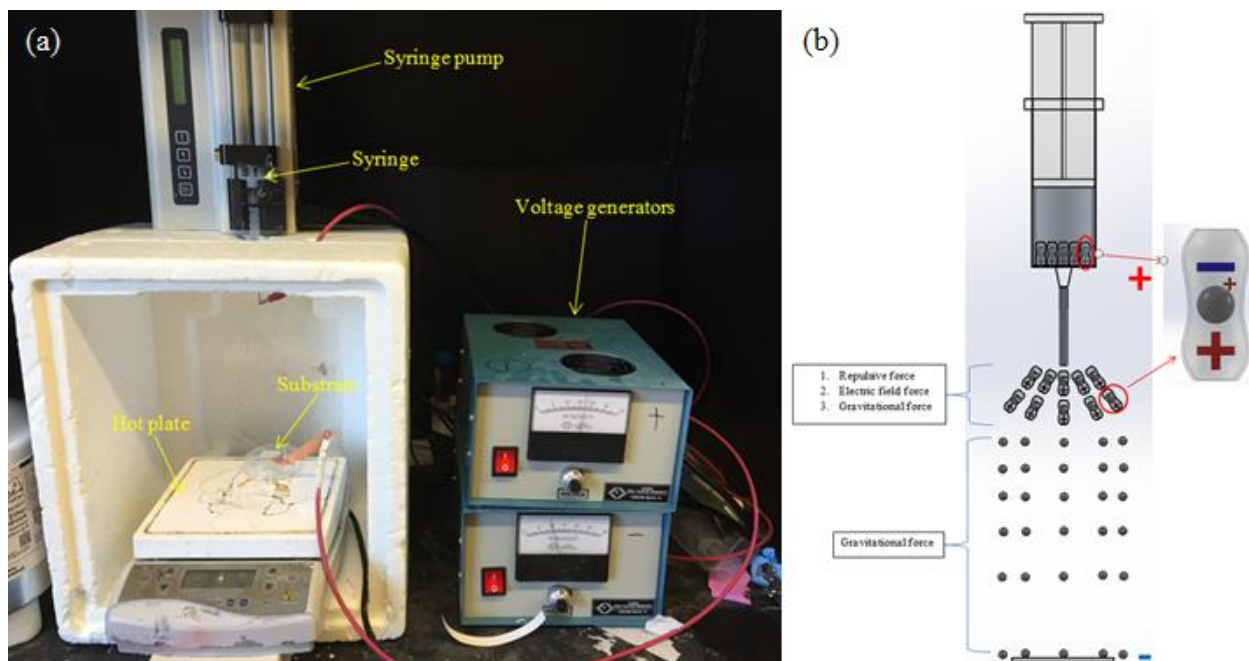


**Figure 5:** (a) Setup of electro-spraying, (b) Schematic of electro-spraying

The whole setup, shown in Figure 5a, consist of a syringe containing  $\text{CuGaO}_2$  colloid, a syringe pump, two voltage generators which are used to polarize the polar organic solvent and build up an electric field between the tip of the nozzle and the substrate that is FTO or ITO. Additionally, if needed, a hot plate can be used to help the evaporation of the solvent to avoid wet particles reaching the substrate.

As presented in schematic, Figure 5b, when the voltages are applied to the polar organic solvent that is ethanol in this experiment, the ethanol molecules will be polarized, and hence the molecules will be aligned. As the  $\text{CuGaO}_2$  colloid flows, at the initial stage, the ethanol molecules, which carry the  $\text{CuGaO}_2$  particles, will form an umbrella-shaped spray as the result of the collaborative effect of repulsive force between polarized

molecules, columbic attraction due to the electric field, and gravitational force. Therefore, the first stage will determine the path that the particles will travel. When the liquid completely vaporizes, the CuGaO<sub>2</sub> nanoparticles do not have charge anymore. Therefore, the nanoparticles undergo free fall and deposit on the substrate.

For the electro-spraying process, there are several experimental parameters can be adjusted. First of all, the applied voltage needs to be greater than the threshold voltage to initiate the spaying process. Also, the flow rate of colloid and the distance between the tip of the nozzle and the substrate should be adjusted appropriately to ensure the liquid can completely vaporize and only the dry CuGaO<sub>2</sub> nanoparticles reach the substrate. For this project, the commonly used parameters are:

- Positive voltage: +17.5 kV
- Negative voltage: -10.0 kV
- Flow rate: 6mL/hr
- Distance: 15.5 cm or 17.5 cm

During the process of deposition, some area of the substrate will be covered by the CuGaO<sub>2</sub> particles first, while other parts of the substrate are still non-covered. However, theoretically, the CuGaO<sub>2</sub> nanoparticles are most likely to go to the uncovered area, since, as shown in Figure 6, the electric field between the tip of nozzle and the substrate is smaller for the covered area than that of the uncovered area. The field strength of the covered area relative to the electric strength of uncovered area, which equals the applied field, can be calculated as following (Moulson, 2003):

$$\vec{E}_{effective} = \vec{E}_0 + \vec{E}_p = \vec{E}_0 - \frac{\vec{P}}{\epsilon_0}$$

$$\vec{P} = \epsilon_0 \chi_e \vec{E}_{effective}$$

$$\vec{E} = \vec{E}_0 - \chi_e \vec{E}_{effective}$$

$$\vec{E}_0 = (1 + \chi_e) \vec{E}_{effective} = \epsilon_r \vec{E}_{effective}$$

where  $\vec{E}_{effective}$  is the effective electric field of the area that is covered by the CuGaO<sub>2</sub> nanoparticles,  $\vec{E}_0$  is the applied field and the field of the uncovered area,  $\vec{E}_p$  is the electric field generated by the alignment of dipoles in the CuGaO<sub>2</sub>,  $\vec{P}$  is the polarization of the dielectric,  $\epsilon_0$  is the permittivity of free space,  $\chi_e$  is the electric susceptibility of CuGaO<sub>2</sub>, and  $\epsilon_r$  ( $\epsilon_r > 1$ ) is the relative permittivity of CuGaO<sub>2</sub>.

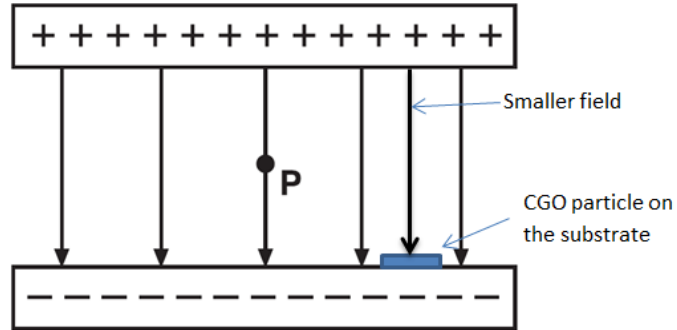


**Figure 6:** Schematic of electric field of the electro-spraying process



Therefore, during the first stage of the spraying process, if assuming every CuGaO<sub>2</sub> particle carries equal amount of charges and all the ethanol molecules are polarized equally, the columbic attraction to the CuGaO<sub>2</sub> particles will be bigger for the area that is uncovered by the CuGaO<sub>2</sub> nanoparticles than the covered area, as calculated below:

$$\begin{aligned}\vec{F}_{covered} &= \vec{E}_{effective} \cdot Q \\ \vec{F}_{uncovered} &= \vec{E}_0 \cdot Q = \epsilon_r \vec{E}_{effective} \cdot Q \\ \vec{F}_{uncovered} &= \epsilon_r \vec{F}_{covered}\end{aligned}$$

where  $\vec{F}_{covered}$  and  $\vec{F}_{uncovered}$  stand for the columbic attraction to the CuGaO<sub>2</sub> particles of the covered area and the uncovered area respectively, and  $Q$  is charges on the CuGaO<sub>2</sub> nanoparticles.

## 2.4 Fabrication of CuGaO<sub>2</sub> thin film through self-assembly

The rational of the self-assembly method comes from the fact that a disordered system tends to become ordered to reduce the total Gibbs free energy of the system. In this case, the Gibbs free energy is comprised of two parts: the surface energy and the volume energy. Thus, the Gibbs free energy of the system can then be expressed as:

$$G_{total} = G_{volume} + G_{surface}$$

The total Gibbs free energy of a system can be reduced by either increasing the volume energy or decrease the surface, because the volume energy,  $G_{volume}$ , is a negative term but the surface energy,  $G_{surface}$ , is a positive term.

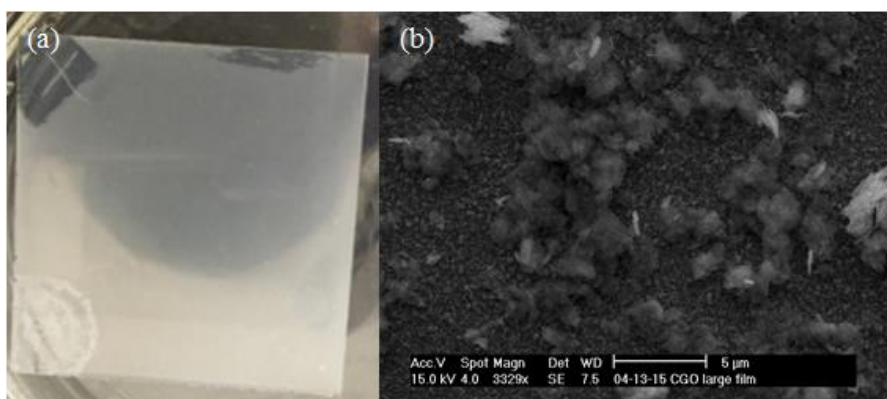
Based on this concept, the CuGaO<sub>2</sub> nanoparticles are mixed with hexane and drop-wisely added into a petri dish containing water and a pre-installed FTO glass at the bottom as the substrate. Because hexane is hydrophobic and its density is lower than that of water, the hexane and CuGaO<sub>2</sub> nanoplates are expected to stay on the top of water. However, hexane is easily volatilized at room temperature. Therefore, eventually only the CuGaO<sub>2</sub> nanoplates will remain on the water surface.

After that, the CuGaO<sub>2</sub> nanoplates tend to self-assemble to reduce the total Gibbs free energy of the system. More specifically, as nanoparticles assembling and forming film, the particle-water interface will reduce; therefore the surface energy of the system will decrease. Once the integrated thin film formed on the surface of water, the petri dish is placed into an oven and heated. As the water vaporizes, the film will precipitate on the FTO substrate.

## Chapter 3: Results and Discussion

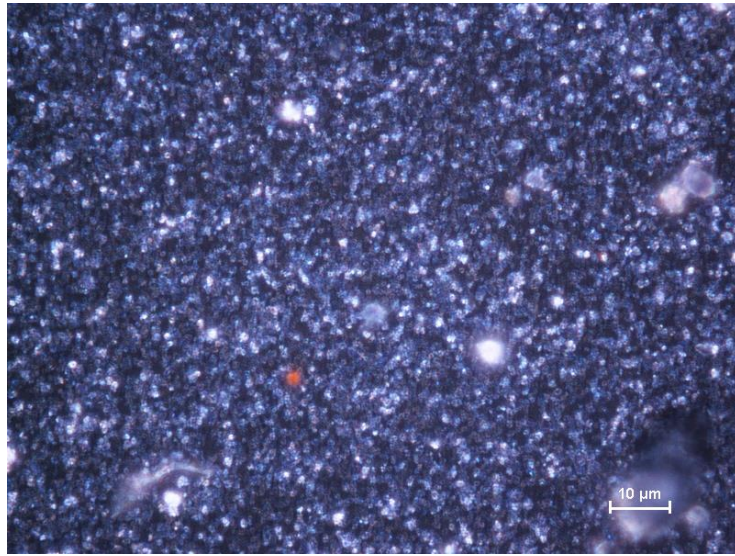
### 3.1 CuGaO<sub>2</sub> thin film fabricated through electro-spraying

Figure 7 shows the first sample made through the electro-spraying process. This sample is made without using colloid. Although a lot of CuGaO<sub>2</sub> nanoparticles are used, appreciable amount of CuGaO<sub>2</sub> are wasted, precipitating at the bottom of the syringe. Therefore, the coverage of the thin film is very poor and the CuGaO<sub>2</sub> nanoparticles form amalgamations.



**Figure 7:** (a) appearance of sample made through electro-spraying, (b) SEM image of the first sample made through electro-spraying (without using CuGaO<sub>2</sub> colloid)

To make the usage of  $\text{CuGaO}_2$  nanoparticles more efficient and solve the problem of amalgamation,  $\text{CuGaO}_2$  colloid is applied for the later samples. As shown in Figure 8, the use of colloid makes the morphology of deposited particle much better, discrete nanoparticles with a few amalgamations.



**Figure 8:**  $\text{CuGaO}_2$  thin film made through electro-spraying by using colloid

The coverage of the thin film is highly determined by the amount of  $\text{CuGaO}_2$  used in the electro-spraying process as shown in Figure 12 (Appendix A). The images in Figure 12 are randomly selected areas of the  $\text{CuGaO}_2$  thin film deposited on the FTO substrate. Then these images are processed, Figure 13 (Appendix B), and the result is listed in Table 1:

**Table 1:** Relationship between the usage of CuGaO<sub>2</sub> particles and coverage

Amount of CuGaO <sub>2</sub> (g)	Coverage (%)
0.007	16.593
0.015	41.156
0.022	75.407
0.030	93.240
0.038	97.019
0.046	99.375
0.054	99.968

Based on the analysis above, if there is enough nanoparticles deposit on the substrate, high quality film that has complete coverage can be fabricated on the substrate. Figure 9 shows an example of the high quality CuGaO<sub>2</sub> thin film on the FTO substrate, and the thickness of the film is about 500 nm. Figure 10 is another example of the high quality film that is deposited on the ITO substrate. Some thin films are heat treated at 350 °C for 1.5 hours with a heating rate of 4 °C/*min*, and the results show that heat treatment can improve the bonding between the CuGaO<sub>2</sub> thin film and the substrate.

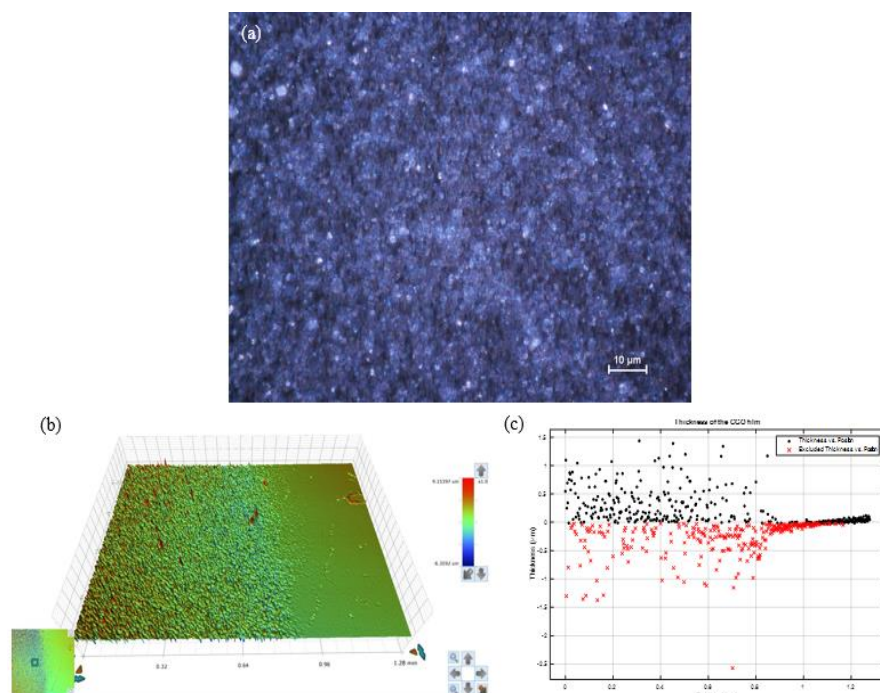


**Figure 9:** (a) Morphology of locally-fully covered thin film (FTO substrate), (b) Simulation of thin film, (c) thickness data of thin film

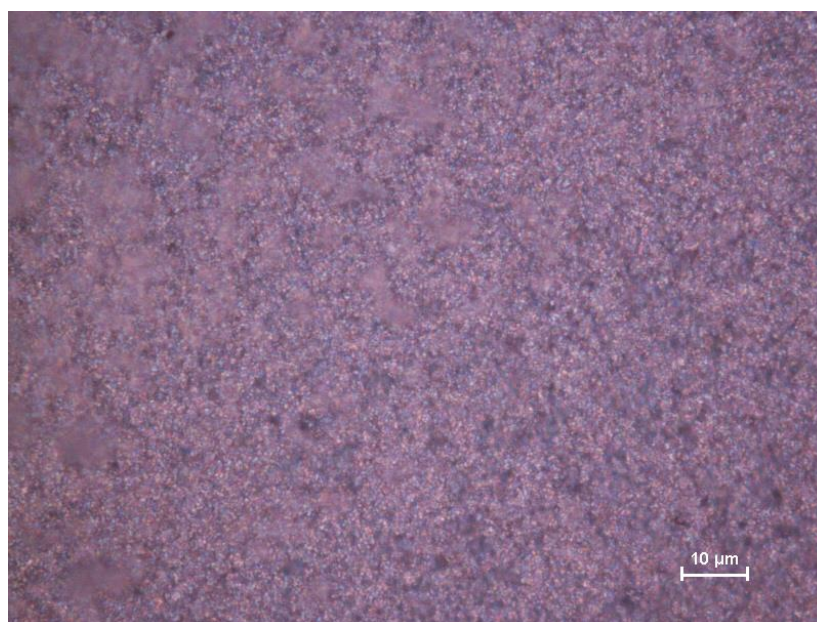


**Figure 10:** Morphology of locally-fully covered thin film (ITO substrate)

However, like other physical deposition process, such as sputtering, the deposited film is not uniform everywhere. Therefore, within a same  $\text{CuGaO}_2$  thin film, although there are some places of desired morphology as shown in Figure 10 and Figure 11, other parts of the film still contain vacancies and holes, because the amount of  $\text{CuGaO}_2$  nanoparticles deposit on the substrate varies from place to place.

Based on the experimental results, the electro-spinning process is a very promising way to fabricate thin film with pre-synthesized nanoparticles, but, with the current setup and experimental parameters, only locally fully covered  $\text{CuGaO}_2$  thin film can be produced, and these locally fully covered  $\text{CuGaO}_2$  thin film cannot be used in solar cell applications because there are still vacancies and holes though out the entire film.

### 3.2 $\text{CuGaO}_2$ thin film fabricated though self-assembly

Self-assembly is actually the first approach that has been used to fabricate the  $\text{CuGaO}_2$  thin film. However, this method is not successful, and some of the  $\text{CuGaO}_2$  thin films made though this method are shown in Figure 11.

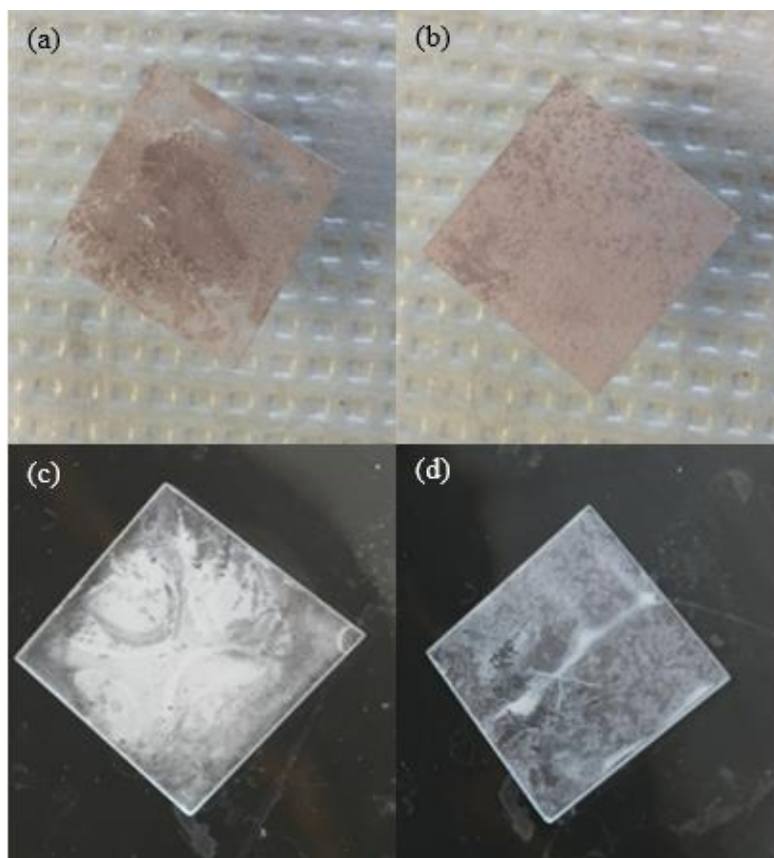


**Figure 11:** (a)-(d) Samples made through self-assembly

There are some difficulties involved in the application of the self-assembly process. First, adding the  $\text{CuGaO}_2$  nanoparticles into water without forming amalgamation and having the nanoparticles evenly distributed on the surface of water are not achievable by manual operation. Second, although the thermodynamics shows that the nanoparticles tend to assemble and form film, the kinetic of this process can be very slow. Third, even though the thin film finally forms on the water surface, it will be very hard to take the film out from the water surface.



## Chapter 4: Conclusion

To accomplish the goal of this research, fabricating CuGaO<sub>2</sub> thin film with an easy and economical approach, first, two mature recipes have been developed to hydrothermally synthesize the CuGaO<sub>2</sub> nanoparticles with different dimensions, diameters of 200 nm and 5  $\mu$ m. Although self-assembly is the first technique applied to fabricate the CuGaO<sub>2</sub> thin film, the results are not successful, because the addition of CuGaO<sub>2</sub> nanoparticles into water leads to non-even distribution of CuGaO<sub>2</sub> nanoparticles on the water surface and particle amalgamations. The second technique, electro-spraying, is able to produce locally fully covered thin films by using the current experiment parameters and CuGaO<sub>2</sub> colloid that is made by adding 0.008 g CuGaO<sub>2</sub> into a mixture of 2.99 mL ethanol and 0.01 mL HCl which has a pH of 1. Additionally, the samples made by electro-spraying show that the quality and coverage of the thin film is highly dependent on the usage of the nanoparticles. Although, thin films made through the electro-spraying process cannot be used for solar cell applications so far, because, as for the entire thin film, there are still vacancies, the electro-spraying technique shows great potential to produce high quality films, providing the spraying process is studied further to achieve better control of the movement of the sprayed particles.

## Chapter 5: Future Work

The electro-spraying technique is definitely a promising approach to fabricate the  $\text{CuGaO}_2$  thin film through physical deposition. There are several approaches that can be applied to further improve the quality of the  $\text{CuGaO}_2$  thin film. First, a spinning substrate can be used to replace the stationary substrate and improve the uniformity of the thin film. Second, the colloid used currently still contains some amalgamations, so the recipe of colloid can be further amended. Third, the path that the nanoparticles take during the first stage of the process needs to be further studied, since it determines where the nanoparticle will finally deposit on the substrate.

## References

- Benko, F. A.; Koffyberg, F. P. (1986), The Optical Interband Transitions of the Semiconductor CuGaO<sub>2</sub>, *Phys. Status Solidi*, 94, 231–234.
- Cario, L., Chavillon, B., Deniard, P., Doussier-Brochard, C., Jobie, S., Odobel, F., Paris, M., and Srinivasan, R. (2008). Tuning the size and color of the p-type wide band gap delafossite semiconductor CuGaO<sub>2</sub> with ethylene glycol assisted hydrothermal synthesis. *Journal of Materials Chemistry*, 18, 5647-5653.
- Draskovic, T. I., Wu, Y., and, Yu, M. (2014). Understanding the Crystallization Mechanism of Delafossite CuGaO<sub>2</sub> for Controlled Hydrothermal Synthesis of Nanoparticles and Nanoplates. *Inorganic Chemistry*, 53(11), pp 5845-5851.
- Fang, Z.-J.; Fang, C.; Shi, L.-J.; Liu, Y.-H.; He, M.-C.(2008), First-principles study of defects in CuGaO<sub>2</sub>, *Chin. Phys. Lett.*, 25, 2997.
- Gillen, R.; Robertson, J. (2011) Band structure calculations of CuAlO<sub>2</sub>, CuGaO<sub>2</sub>, CuInO<sub>2</sub>, and CuCrO<sub>2</sub> by screened exchange, *Phys. Rev. B*, 84, 035125.
- Kassap, S.O., Principles of Electronic Materials, *University of Saskatchewan Canada*, 2012, pp388-392.
- Ji,Z., Natu, G., Yu, M., Wu, Y. (2012), p-Type Dye-sensitized Solar Cell Based on Delafossite CuGaO<sub>2</sub> Nanoplates with Situation Photovoltage Exceeding 460 mV, *J. Phys. Chem. Lett.*, 3(9), pp 1074-1078
- Levine, Ira N. (2001). Physical Chemistry (5th ed.). *Boston: McGraw-Hill*. ISBN 0-07-231808-2., p. 955
- Nie, X.; Wei, S.-H.; Zhang, S. B.(2002), S.B., Bipolar Doping and Band-Gap Anomalies in Delafossite Transparent Conductive Oxides, *Phys. Rev. Lett.* , 88, 066405.
- Ueda, K.; Hase, T.; Yanagi, H.; Kawazoe, H.; Hosono, H.; Ohta, H.; Orita, M.; Hirano, M. J. (2001), Epitaxial growth of transparent p-type conducting CuGaO<sub>2</sub> thin films on sapphire (001) substrate by pulsed laser deposition, *Appl. Phys.*, 89, 1790–1793.

Appendix A: Microscopic image of CuGaO<sub>2</sub> thin film

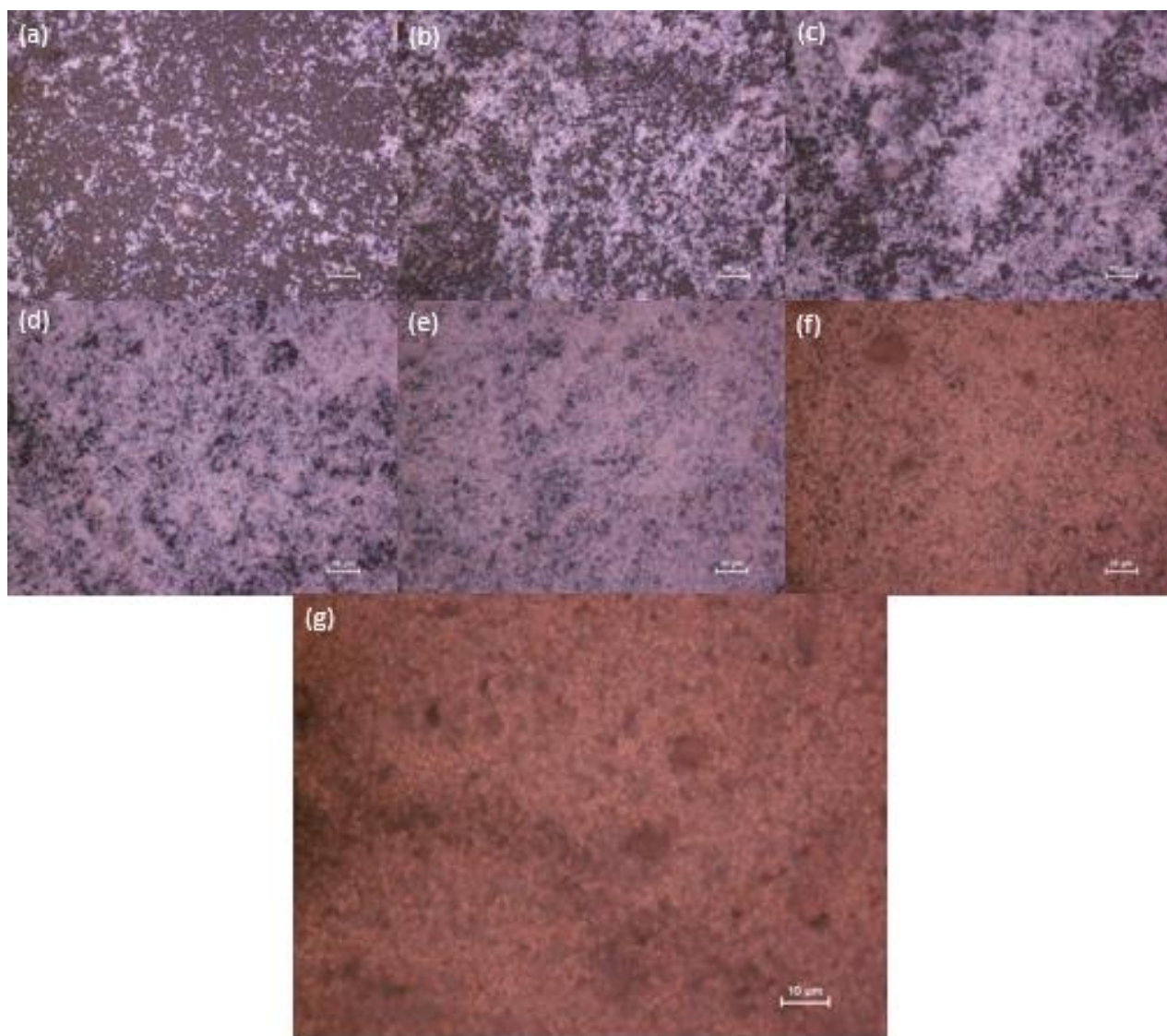


**Figure 12:** Morphology of thin film with different amount of CuGaO<sub>2</sub> nanoparticles, (a) 0.007g, (b) 0.015 g, (c) 0.022g, (d) 0.030 g, (e) 0.038g, (f) 0.046 g, (g) 0.054 g

## Appendix B: Image analysis of Figure 13

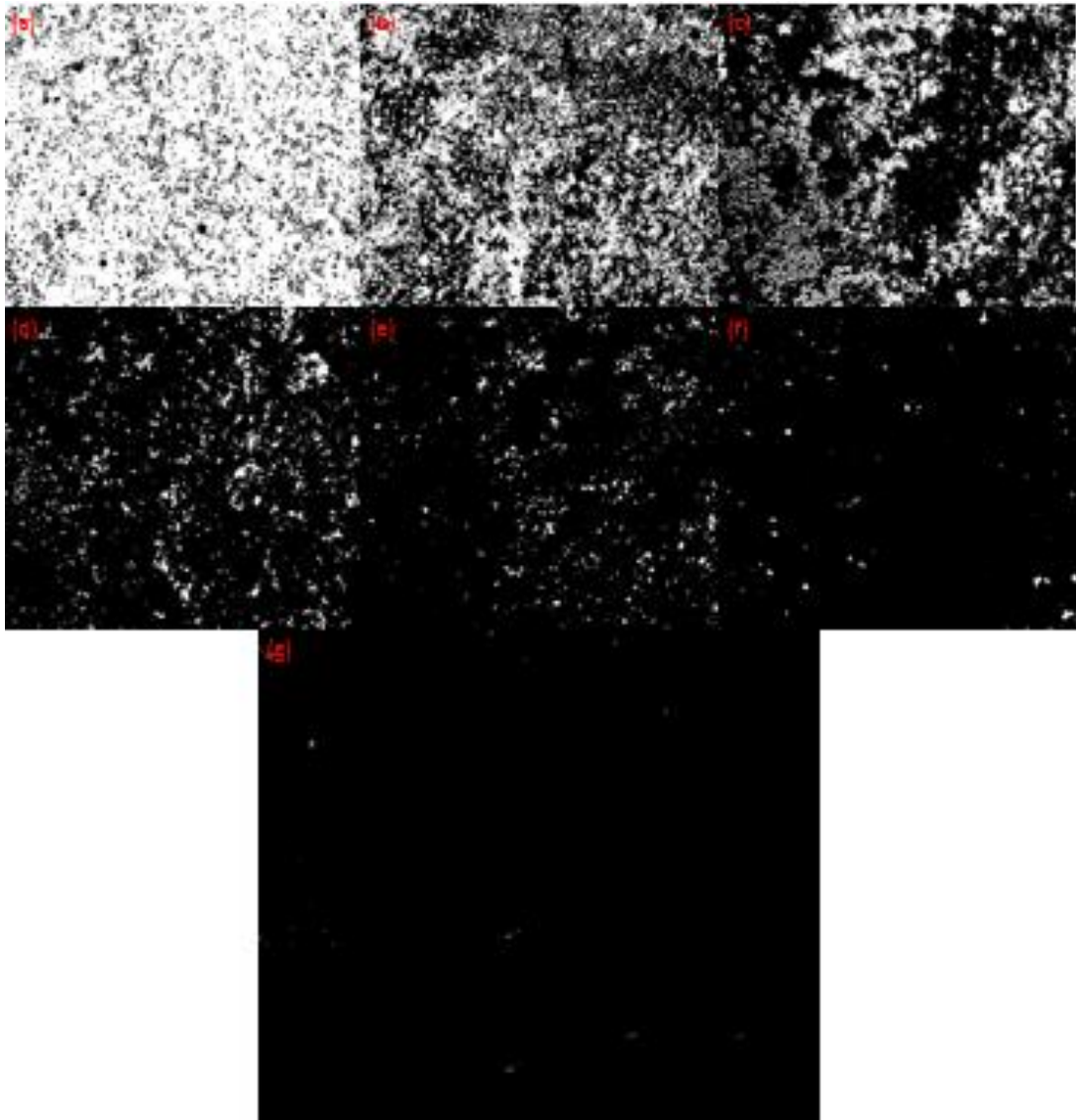


**Figure 13:** Image process of Figure 13. (black: covered, white: uncovered)